0026-895X/10/7706-953–960$20.00
MOLECULAR PHARMACOLOGY
Copyright © 2010 The American Society for Pharmacology and Experimental Therapeutics
Mol Pharmacol 77:953–960, 2010

Vol. 77, No. 6
63636/3589044
Printed in U.S.A.

Genetic and Functional Analysis of Human P2X5 Reveals a Distinct Pattern of Exon 10 Polymorphism with Predominant Expression of the Nonfunctional Receptor Isoform

Smita Kotnis, Brendan Bingham, Dmitry V. Vasilyev, Scott W. Miller, Yuchen Bai, Sarita Yeola, Pranab K. Chanda, Mark R. Bowlby,[1] Edward J. Kaftan, Tarek A. Samad, and Garth T. Whiteside

Pfizer Global Research and Development, Princeton, New Jersey

Received January 19, 2010; accepted March 11, 2010

ABSTRACT

P2X5 is a member of the P2X family of ATP-gated nonselective cation channels, which exist as trimeric assemblies. P2X5 is believed to trimerize with another member of this family, P2X1. We investigated the single-nucleotide polymorphism (SNP) at the 3′ splice site of exon 10 of the human P2X5 gene. As reported previously, presence of a T at the SNP location results in inclusion of exon 10 in the mature transcript, whereas exon 10 is excluded when a G is present at this location. Our genotyping of human DNA samples reveals predominance of the G-bearing allele, which was exclusively present in DNA samples from white American, Middle Eastern, and Chinese donors. Samples from African American donors were polymorphic, with the G allele more frequent. Reverse transcription-polymerase chain reaction analysis of lymphocytes demonstrated a 100% positive correlation between genotype and P2X5 transcript. Immunostaining of P2X1/P2X5 stably coexpressing cell lines showed full-length P2X5 to be expressed at the cell surface and the exon 10-deleted isoform to be cytoplasmic. Fluorometric imaging-based pharmacological characterization indicated a ligand-dependent increase in intracellular calcium in 1321N1 astrocytoma cells transiently expressing full-length P2X5 but not the exon 10-deleted isoform. Likewise, electrophysiological analysis showed robust ATP-evoked currents when full-length but not the exon 10-deleted isoform of P2X5 was expressed. Taken together, our findings indicate that most humans express only a nonfunctional isoform of P2X5, which is in stark contrast to what is seen in other vertebrate species in which P2X5 has been studied, from which only the full-length isoform is known.

P2X receptors belong to the family of nonselective cation channels gated by extracellular ATP (Burnstock, 2006; Surprenant and North, 2009). To date, seven P2X receptors have been cloned, denoted P2X1–P2X7 (MacKenzie et al., 1999). P2X receptors form trimeric assemblies (Kawate et al., 2009) with both homomeric and heteromeric forms having been described previously (Virginio et al., 1998; Haines et al., 1999; Cockayne et al., 2005; Guo et al., 2007; Nicke, 2008). P2X5 is widely expressed in immune and nervous system tissue (Lê et al., 1997) and heart and skeletal muscle (Collo et al., 1996; Garcia-Guzman et al., 1996; Cox et al., 2001; North, 2002; Ryten et al., 2002; Guo et al., 2008; Musa et al., 2009).

Among the known human P2X5 splice variants is a polymorphism for exon 10. The 22 amino acids encoded by exon 10, including the carboxyl terminus of the extracellular ATP-binding site (Hansen et al., 1997) and the amino terminus of the second transmembrane domain (Fig. 1A), are important to ion channel function. Absence of these residues results in a nonfunctional protein that is prone to aggregation (Lê et al., 1997; Bo et al., 2003; Duckwitz et al., 2006). The human polymorphism for exon 10 is in fact a polymorphism for functional P2X5 receptor.

The human P2X5 exon 10 polymorphism arises from a single-nucleotide polymorphism (SNP) at the 3′ splice site of exon 10 (Fig. 1B). The original P2X5 cDNA cloned from human brain lacks an exon 10 sequence (Lê et al., 1997),

[1] Current affiliation: Pain and Migraine Research, Merck Research Labs, West Point, Pennsylvania.

Article, publication date, and citation information can be found at http://molpharm.aspetjournals.org.
doi:10.1124/mol.110.063636.

ABBREVIATIONS: SNP, single-nucleotide polymorphism; FLIPR, fluorometric imaging plate reader; $\alpha\beta$-me-ATP, α-β-methyl-ATP; PPADS, pyridoxal-phosphate-6-azophenyl-2′,4′-disulfonic acid; GFP, green fluorescent protein; BCC, basal cell carcinoma; SCC, squamous cell carcinoma; RT, reverse transcription; PCR, polymerase chain reaction; bp, base pair(s); PAGE, polyacrylamide gel electrophoresis; TNP, 2′,3′-*O*-(2,4,6-trinitrophenyl); TM, transmembrane.

similar to most human P2X5 GenBank deposits (Bo et al., 2003). Only conservative amino acid substitutions in the exon 10 sequence (K330R, S332N, I337V and I340V, and L344V) are seen in comparisons of species spanning mammals, birds, amphibians, and fish (Garcia-Guzman et al., 1996; Jensik et al., 2001; Ruppelt et al., 2001; Diaz-Hernandez et al., 2002; Bo et al., 2003). Human and rat P2X5 exon 10 seem to be functionally equivalent, despite three amino acid differences (Lê et al., 1997; Bo et al., 2003). Among the reference sequences in the Ensembl database, only that of humans contains a G at the P2X5 exon 10 3′ SNP position, suggesting that P2X5 transcripts of other species contain this exon (Fig. 1C). Interrogation of the dbSNP and Hapmap databases reveals insufficient data to determine the frequency or ethnic distribution of this human SNP (International HapMap Consortium, 2003), leaving unclear the extent to which human ATP signaling is mediated by P2X5 function.

P2X1, a frequently observed heteromeric partner of P2X5 (Lê et al., 1997, 1999; Torres et al., 1998; Haines et al., 1999; Bo et al., 2003; Duckwitz et al., 2006), is widely expressed, including in central nervous system and cardiac tissue and smooth muscle (North, 2002; Ashour et al., 2006; Musa et al., 2009). Heterologous coexpression of rat P2X1 and P2X5 results in biophysical and pharmacological properties distinct from those observed for each of the receptors expressed separately. Expressed alone, rat P2X1 gives a large, rapidly desensitizing current in response to ATP or $\alpha\beta$-me-ATP, whereas rat P2X5 gives small, nondesensitizing currents (Torres et al., 1998; Haines et al., 1999; Lê et al., 1999). By contrast, coexpression of these two receptors results in biphasic ATP-evoked currents typified by rapid decay from the peak current to a prolonged plateau (Torres et al., 1998; Haines et al., 1999) and slowly desensitizing $\alpha\beta$-me-ATP-evoked currents (Torres et al., 1998; Lê et al., 1999). Mouse cortical astrocytes express both P2X1 and P2X5 and produce ATP-evoked currents that are biphasic and sensitive to inhibition by the purinergic receptor blocker pyridoxal-phosphate-6-azophenyl-2′,4′-disulfonic acid (PPADS), properties that are characteristic of P2X1/P2X5 heteromeric channels (Lalo et al., 2008). Expression of the full-length isoform of human P2X5 in the absence of P2X1 results in robust ATP-mediated currents, which is similar to heterologous expression of chicken and bullfrog, but not rodent, P2X5 (Bo et al., 2003; Duckwitz et al., 2006).

We aimed to characterize human P2X5 exon 10 polymorphism by genotyping DNA from a sampling of the human population, spanning four races: white American, African American, Middle Eastern, and Chinese. We coupled this genetic survey with a comparative analysis of the two human P2X5 exon 10 isoforms, investigating electrophysiology and the pharmacology of ligand-mediated calcium signaling. In view of the prominence of heteromeric assemblages of P2X receptors, we also extended our analysis to the immunocytochemical and pharmacological characterization of cells coexpressing human P2X1 with each of the P2X5 exon 10 isoforms.

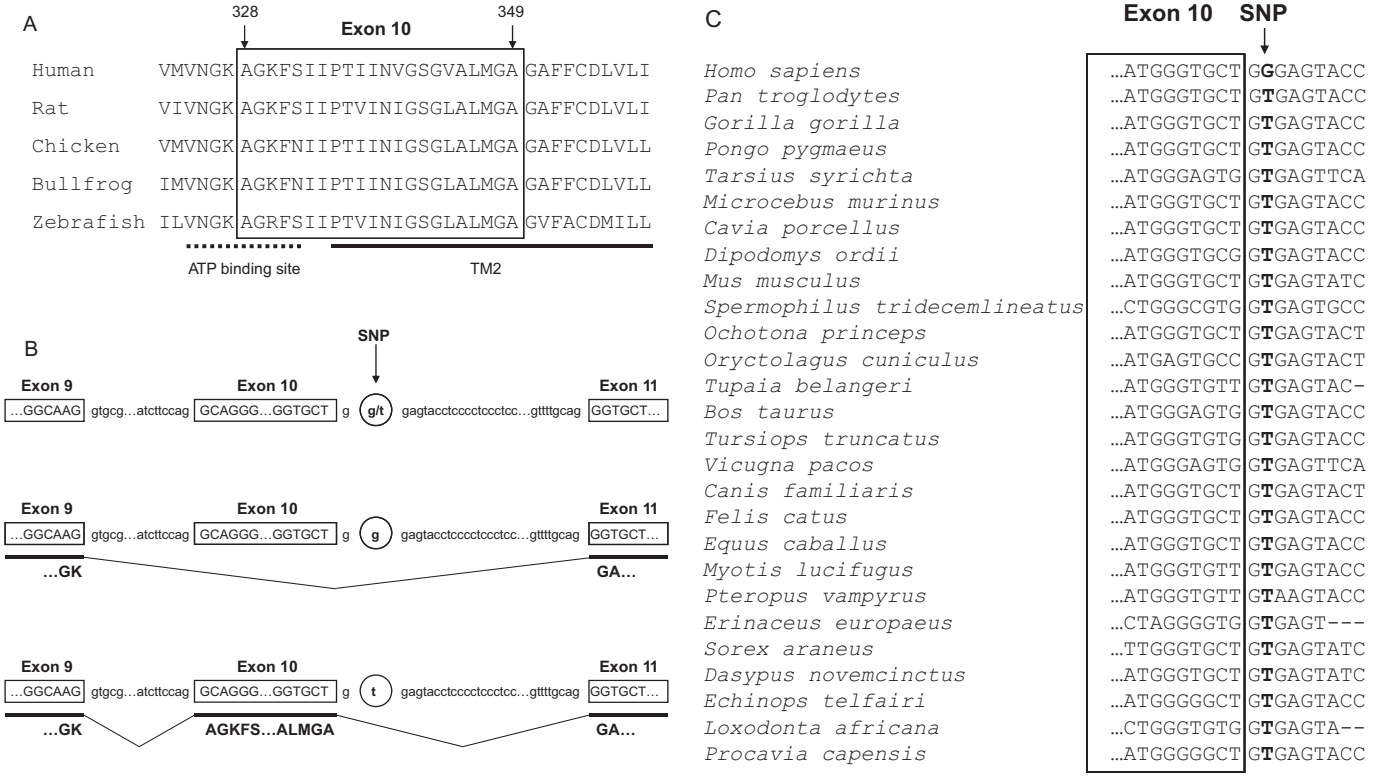

Fig. 1. P2X5 exon 10 sequence. A, comparison of P2X5 amino acid sequence in the region of exon 10 reveals only conservative amino acid differences among diverse vertebrate species. Amino acid numbering is according to human sequence. Exon 10-encoded sequence is boxed. The putative ATP binding site (dashed line) and putative second transmembrane domain (TM2; solid line) are underlined. B, a SNP determines the splicing of human P2X5 exon 10. Polymorphism at the 3′ splice site of exon 10 results in exclusion of exon 10 from the mature transcript when a G is present or inclusion when a T is present. C, in the Ensembl reference genome assembly, a G is present at the human P2X5 exon 10 3′ SNP position. Reference sequences for 26 other eutherian mammals have a T at this position. Exon 10 sequence is boxed.

Materials and Methods

Genotyping. Taqman allelic discrimination assay was performed by using ABI TaqMan SNP genotyping assay ID C_8728453_10 and the ABI instrument 7900HT fast real-time PCR system (Applied Biosystems, Foster City, CA). PCR amplifications were performed in duplicate with 20 ng of template genomic DNA, according to the manufacturer's protocol. All reactions assessed the SNP at the 3′ intronic splice site of human P2X5 exon10 (National Center for Biotechnology Information SNP database ID rs891746). Data from the endpoint reads were analyzed with SDS2.3 software (Applied Biosystems). Human genomic DNA samples included 50 samples (Bioserve Biotechnologies, Laurel, MD) from white American donors, of which 46 produced interpretable signals, and 30 samples (Coriell Institute for Medical Research, Camden, NJ) consisting of 10 each from African American, Middle Eastern, and Chinese donors. DNA derived from A431, a human squamous cell carcinoma (SCC) cell line (European Collection of Cell Cultures 85090402), was also genotyped. Twenty-seven eutherian mammal reference genome sequences in the region of the interrogated SNP site were downloaded from the Ensembl database for alignment.

P2X Ligands. Purinergic agonists ATP and $\alpha\beta$-me-ATP and antagonists TNP-ATP, suramin, and PPADS were purchased from Sigma-Aldrich (St. Louis, MO) (Burnstock, 2006; Surprenant and North, 2009).

DNA Constructs. Plasmids containing cDNA constructs encoding human P2X1 (NM_002558) and human P2XΔ5$^{328–349}$ (NM_002561; the P2X5 isoform lacking exon 10 sequence encoding amino acids 328–349) were purchased from Origene (Rockville, MD). Coding sequences were PCR-amplified, using primers that included the addition of a Kozak sequence upstream of the start codon, followed by subcloning into the pCR2.1-TOPO vector (Invitrogen, Carlsbad, CA). Human P2X5FL, the full-length isoform of P2X5, was constructed by excising 370 bp from P2X5Δ$^{328–349}$/pCR2.1-TOPO by restriction digestion with BmgB1 (position 963 of coding sequence) and Acc65I (vector sequence, downstream of cloning site), and replacing it with an exon 10-containing, 436-bp fragment synthesized by oligonucleotide-mediated synthesis (Cherry et al., 2008). Twenty-four overlapping DNA primers covering the 436-bp fragment were designed with UpGene synthesis software (University of Pittsburgh, Pittsburgh, PA). All constructs were subcloned into the vector pCDNA3.1(+). The vector containing the P2X1 construct carried a phleomycin (Zeocin)-selectable marker, and the P2X5FL and P2X5Δ$^{328–349}$ constructs each carried a hygromycin-selectable marker.

Stably Expressing Cell Lines. All cell culture reagents were from Invitrogen. Stable cell lines expressing human P2X1 were generated by transfecting human astrocytoma cell line 1321N1 (European Collection of Cell Cultures 86030402), which has been shown previously to be ATP-unresponsive (Jarvis et al., 2002; Nagata et al., 2009), with the P2X1/pcDNA3.1 construct by using Lipofectamine 2000 (Invitrogen). Cells were maintained in Dulbecco's modified Eagle's medium containing 10% fetal bovine serum, 1% penicillin/streptomycin, and 1% L-glutamine, to which phleomycin (40 μg/ml) was added for selection of P2X1 transfectant clones. P2X1 stable cell lines were evaluated on the basis of their ability to mobilize calcium in response to ATP in a fluorometric imaging plate reader (FLIPR; Molecular Devices, Sunnyvale, CA)-based assay. Stably coexpressing cell lines (P2X1/P2X5FL and P2X1/ P2X5Δ$^{328–349}$) were obtained by transfecting the P2X1 stable cell line with P2X5FL/pcDNA3.1 and P2X5Δ$^{328–349}$/pcDNA3.1 DNA, respectively. Positive clones were selected in cell culture medium containing hygromycin (100–300 μg/ml). The double stable clones were first evaluated for P2X5 expression by RT-PCR, and expression was confirmed by Western blot analysis. Coexpression of P2X5 with P2X1 was evaluated in stable cell lines rather than with transient coexpression, which can be subject to multiple sources of variation. Using the P2X1 stably expressing cell line as the host for transfection of the P2X5 variants removes P2X1 expression as a source of variability.

Transient Expression. P2X5 receptor isoforms (P2X5FL/pcDNA3.1 or P2X5Δ$^{328–349}$/pcDNA3.1) were transiently transfected into 1321N1 cells by using Lipofectamine 2000. For electrophysiological recordings, cotransfection with the GFP-encoding plasmid pEGFP-N1 (Clontech, Mountain View, CA) was performed; cells displaying green fluorescence were patched manually.

RT-PCR. Total RNA was prepared from cells in culture for 48 to 72 h by using the RNeasy mini kit (QIAGEN, Valencia, CA). RNA (2 μg) was reverse-transcribed by using oligo(dT) primers and SuperScript II enzyme (Invitrogen). Human P2X5 primers (forward: 5′-CACTATTCTTTTAGCCGTCTGGAC-3′; and reverse: 5′-TTCTGACTGCTGCTTCCACGCTTC-3′) were used to amplify fragments of 461 and 395 bases from P2X5FL and P2X5Δ$^{328–349}$, respectively.

Western Blot Analysis. Stably expressing cell lines were plated for 48 to 72 h and washed three times with phosphate-buffered saline. Cells extracted were prepared by using lysis buffer containing 50 mM Tris-HCl, pH 7.5, 0.5% Triton X-100, and complete mini-protease inhibitor cocktail (Roche Diagnostics, Pleasanton, CA). Cells were scraped, and mechanical disruption of the cells was achieved by several passages through a syringe attached to a 23-gauge hypodermic needle. After a 30-min incubation on ice, lysates were spun, and the supernatant collected was measured for protein concentration with the BCA protein assay kit (Novagen-EMD Chemicals, Gibbstown, NJ). NuPAGE sample buffer and NuPAGE reducing agent (Invitrogen) were added to the cell extract. Samples were loaded onto NuPAGE 10% Bis-tris gel. Western blotting was performed by using reagents from the one-step Western blotting kit (GenScript USA, Inc., Piscataway, NJ), according to the manufacturer's instructions. Blots were probed with goat anti-P2X1 or rabbit anti-P2X5 from Santa Cruz Biotechnology, Inc. (Santa Cruz, CA).

Immunocytochemistry. Cells cultured on polylysine-coated coverslips were fixed with IC fixation buffer (4% paraformaldehyde in phosphate-buffered saline, pH 7.3; Invitrogen) and blocked with Tris-buffered saline, 0.5% Triton-X-100, and 2% normal donkey serum for 30 min at room temperature. Stably expressing cells were incubated with primary antibodies, goat anti-P2X1 (Y-14) and rabbit anti-P2X5 (H-90) (Santa Cruz Biotechnology, Inc.) (overnight at 4°C). A431 cells were incubated with rabbit anti-P2X5 (H-90) and mouse anti-CD29 (Sigma-Aldrich) (overnight at 4°C). After washing, stably expressing cells were incubated with donkey secondary antibodies, anti-rabbit Alexa Fluor 488, and anti-goat Alexa Fluor 633. A431 cells were incubated with anti-rabbit Alexa Fluor 488 and anti-mouse Alexa Fluor 594; to counterstain nuclei, Hoechst 33258 (Invitrogen) was included in the secondary antibody incubation at a final concentration of 10 μg/ml. Coverslips were washed and mounted by using ProLong Gold anti-fade mounting solution (Invitrogen). Images were obtained with a Leica (Wetzlar, Germany) SP5 confocal microscope.

Intracellular Calcium Measurements. Cells were seeded at a density of 20,000 per well and cultured overnight in 384-well tissue culture-treated plates. Culture medium was aspirated, and cells were incubated for 1 h with 4 μM Fluo-4 (Invitrogen) followed by a brief wash with Hanks' balanced salt solution. Antagonist compounds were diluted in 100% dimethyl sulfoxide; agonists were diluted in water (concentration range 1.6 nM to 100 μM for EC_{50} determination of agonists). All assays were performed on the FLIPR3.1 (Molecular Devices). Agonists were added by FLIPR immediately before data capture. Antagonists were added by FLIPR and incubated for 10 min before agonist addition (at the EC_{80}; 200 nM) and data capture. Data were captured as the quantity maximum–minimum between the point of agonist addition and just after the assay peak. FLIPR data were analyzed with Prism 5 (GraphPad Software Inc., San Diego, CA).

Electrophysiology. All recordings were made from 1321N1 GFP-positive cells in whole-cell voltage-clamp configuration at 23°C. The extracellular solution was Hanks' balanced salt solution (Invitrogen): 138 mM NaCl, 4.17 mM $NaHCO_3$, 0.34 mM Na_2HPO_4, 5.3 mM

KCl, 0.44 mM KH_2PO_4, 1.26 mM $CaCl_2$, 0.49 mM $MgCl_2$, 0.41 mM $MgSO_4$, and 5.5 mM glucose, supplemented with HEPES to 10 mM. Pipette resistance was 2 to 3 MΩ when filled with the intracellular solution consisting of 100 mM K-gluconate, 30 mM KCl, 10 mM NaCl, 0.5 mM $CaCl_2$, 10 mM EGTA, and 10 mM HEPES 10, pH 7.3 with KOH. Cells were held at −70 mV, and currents were evoked by a fast microperfusion (micromanifold; ALA Scientific, Westbury, NY) application of 30 μM ATP. Whole-cell currents were filtered at 1 to 2 kHz, collected by a MultiClamp 700A amplifier, and digitized at 5 kHz by using DigiData 1322A and pClamp9 software (all from Molecular Devices). Data were analyzed with Clampfit (Molecular Devices) and Origin 7.0 (OriginLab Corp., Northampton, MA). Data were expressed as mean ± S.E.M. Log-transformed data were analyzed by one-way analysis of variance, followed by post hoc testing (Bonferroni) of all pairwise comparisons.

Results

Human P2X5 Exon 10 SNP Analysis. The P2X5 exon 10 SNP was examined first in a set of genomic DNA samples obtained from Bioserve Technologies. All 46 samples analyzed were found to produce signal only for the G-containing allele, which encodes the $P2X5\Delta^{328–349}$ isoform of P2X5 (Fig. 2A), indicating the donors to be GG homozygotes. Positive control samples, consisting of synthetic DNA fragments identical in sequence to the G- and T-containing alleles, were used to validate allelotypes. After SNP analysis, each of these control samples gave the expected result, as did control samples consisting of an equal mix of G- and T-containing fragments (data not shown).

Because we found neither GT heterozygotes nor TT homozygotes among the first 46 samples, all of which were from white American donors, we then expanded our analysis to include additional samples, 10 each from African American, Middle Eastern, and Chinese donors. All of the Middle Eastern and Chinese samples proved to be GG homozygotes. Six of the African American samples were GT heterozygotes, and one was a TT homozygote, whereas three were GG homozygotes (Fig. 2B).

In addition, the human squamous cell carcinoma-derived cell line A431, in which P2X5 expression has been reported previously (Greig et al., 2003), was also genotyped and found to be homozygous for the G-bearing allele of the P2X5 exon 10 SNP (data not shown).

Correlation of P2X5 Genotype and Mature Transcript. Lymphocyte cell lines, derived from blood samples collected from a subset of the individuals that were genotyped, were obtained from the Coriell Institute for Medical Research. Specifically, cells were obtained from one Chinese, six African American, and two Middle Eastern donors. RT-PCR analysis was performed with P2X5 PCR primers that span the exon 10 region. Amplification of a 395-bp fragment indicated expression of a P2X5 transcript lacking exon 10, whereas a 461-bp fragment was amplified from P2X5FL. This analysis revealed a 100% positive correlation between genotype and transcript expression. GG individuals expressed only the shorter transcript, the TT individual expressed only the full-length transcript, and heterozygotes expressed both transcripts (Fig. 2B, bottom).

RT-PCR analysis of cultured A431 cells revealed the presence of a 395-bp amplicon (data not shown), indicating transcription of only the $P2X5\Delta^{328–349}$ isoform, consistent with our genotyping data for this cell line.

Western and Immunocytochemical Analysis of P2X1 and P2X5 Expression. A P2X1 stably expressing 1321N1 cell line was generated; P2X1 expression was confirmed by RT-PCR (data not shown) and Western blotting. This cell line

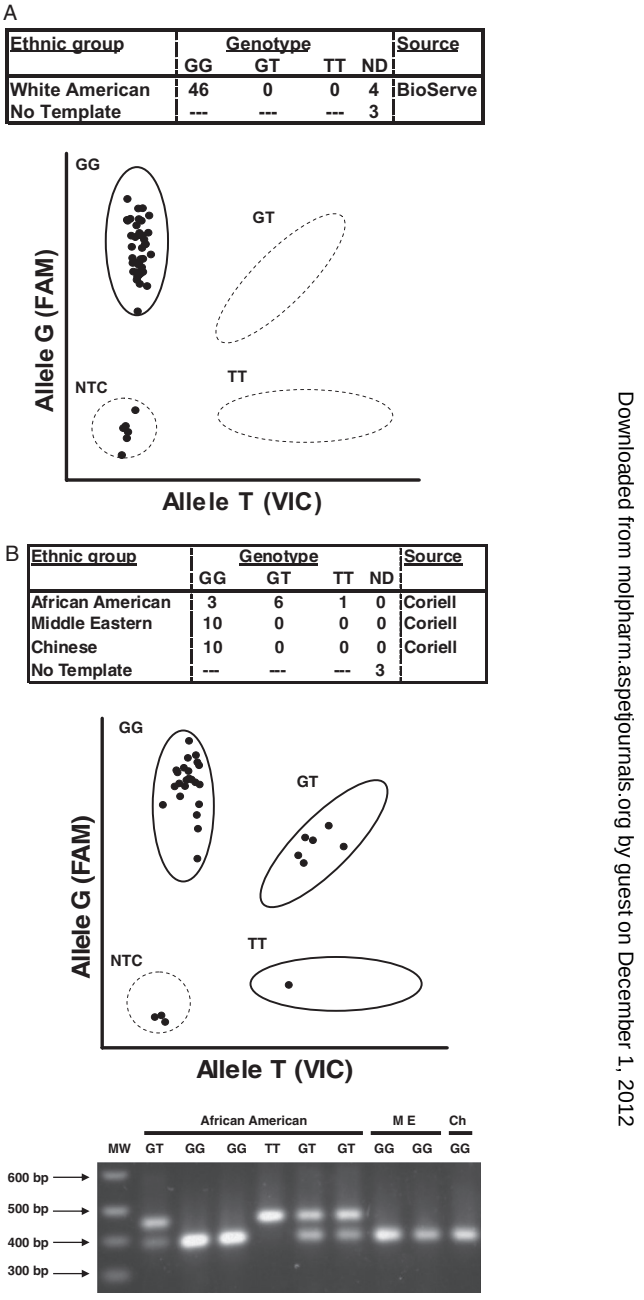

Fig. 2. Analysis of the human P2X5 exon 10 SNP. Genotyping of human genomic DNA samples was performed. Allelic clusters are circled, including no template control (NTC). A, analysis of genomic DNA samples obtained from Bioserve Biotechnologies from a set of white American donors resulted in the detection of only GG homozygotes. B, top, analysis of genomic DNA samples obtained from the Coriell Institute for Medical Research from African American, Middle Eastern, and Chinese donors resulted in the detection of only GG homozygotes among the Middle Easterners and Chinese. Samples from African American donors resulted in the detection of three GG homozygotes, six GT heterozygotes, and one TT homozygote. Bottom, RT-PCR analysis using P2X5 primers spanning exon 10 revealed that homozygotes expressed only one transcript, corresponding to the transcription product expected from the exon 10 splicing event, and heterozygotes expressed both transcripts. The molecular weight marker (MW) and donor's genotype (GG, GT, or TT) are as indicated. ME, Middle Eastern; Ch, Chinese.

was then transfected with plasmids encoding each of the P2X5 exon 10 isoforms, and stably coexpressing cell lines were derived. Expression of P2X1 protein in the P2X1 cell line and the P2X1/P2X5 coexpressing cell lines was confirmed by the presence of a band at 53 kDa on a Western-blotted SDS-PAGE gel (Fig. 3A, left). In the coexpressing cell lines, bands indicating P2X5 protein expression were also observed upon Western blotting. The full-length P2X5 band migrates at approximately 60 kDa in P2X1/P2X5FL stables (Fig. 3A, right); the protein detected in the P2X1/P2X5Δ$^{328–349}$ cell line is at a slightly lower molecular mass, consistent with the absence of the 22 amino acids encoded by exon 10.

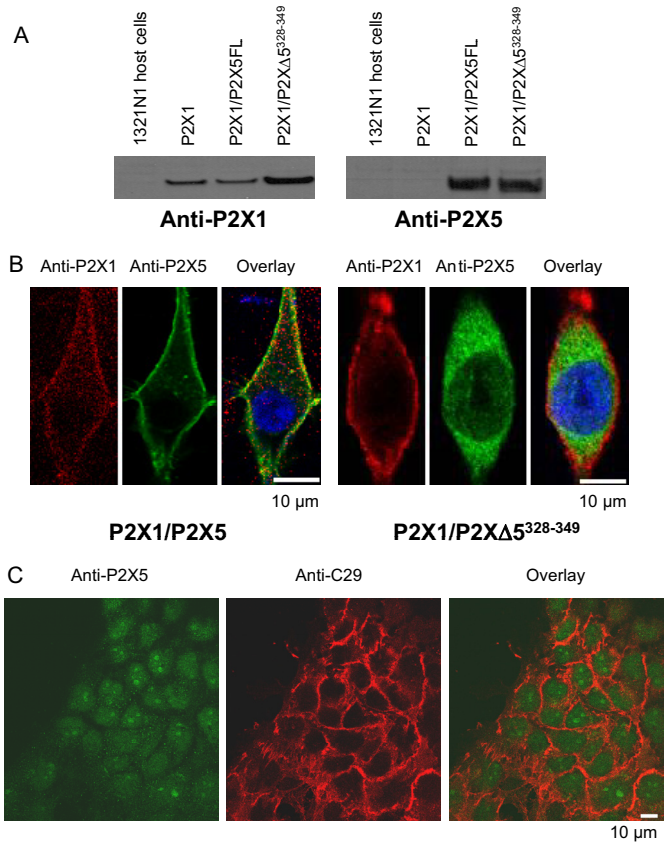

Fig. 3. Western blot and immunocytochemical analysis of human P2X1 and P2X5. A, Western blot analysis indicating the presence of P2X1 protein in the P2X1 stable cell line and the P2X1/P2X5FL and P2X1/P2X5Δ$^{328–349}$ double-stable cell lines (left) and P2X5 protein expression in the P2X1/P2X5FL and P2X1/P2X5Δ$^{328–349}$ double-stable cell lines (right). B, immunocytochemical analysis indicating P2X1 (red) and P2X5 (green) staining in the P2X1/P2X5FL and P2X1/P2X5Δ$^{328–349}$ double-stable cell lines and their spatial overlap (yellow). Nuclear staining was with Hoechst 33258 (blue). Scale bars, 10 μm. C, immunocytochemical analysis indicating P2X5 (green) and CD29 (red) staining in A431 human squamous carcinoma cells. Scale bar, 10 μm.

Examined by immunofluorescence, P2X1 (Fig. 3B, red) expression was localized mainly to the cell surface in both the P2X1/P2X5FL and the P2X1/P2X5Δ$^{328–349}$ cell lines. In the P2X1/P2X5FL cell line, P2X5 staining (Fig. 3B, green) also displayed a cell-surface distribution and substantial overlap (Fig. 3B, yellow) with P2X1 protein expression (Fig. 3B, left). In contrast, P2X5 expression in the P2X1/P2X5Δ$^{328–349}$ cells was cytoplasmic, indicating that the absence of the exon 10-encoded amino acids substantially alters the distribution of this protein.

Immunostaining of the A431 cell line showed predominant cytoplasmic localization of P2X5, consistent with the genetic and molecular determination of P2X5Δ$^{328–349}$ expression in these cells. Costaining for the cell-surface protein CD29 revealed no detectable overlap with P2X5 staining (Fig. 3C).

Pharmacological Analysis of 1321N1 Cells Expressing P2X1 and P2X5 Isoforms. To assess the physiological consequences of the expression of the P2X5 exon 10 isoforms in the context of coexpression with P2X1, we measured the potency of the agonists ATP and αβ-me-ATP in a FLIPR-based calcium assay in P2X1 stably expressing and P2X1/P2X5 stably coexpressing 1321N1 cells (Table 1 and Fig. 4). Parental 1321N1 cells did not produce an increase in intracellular calcium in response to these agonists applied up to a concentration of 100 μM (Table 1). In cells expressing P2X1 alone, EC_{50} values of 0.057 and 0.160 μM were observed for ATP and αβ-me-ATP, respectively. In cells coexpressing P2X1 and P2X5FL, the EC_{50} values for ATP and αβ-me-ATP were shifted less than 2-fold from those of cells expressing only P2X1. Likewise, coexpression of P2X5Δ$^{328–349}$ with P2X1 produced only minor changes in the concentration response curve compared with cells coexpressing P2X1 and P2X5FL (Table 1 and Fig. 4).

Transient transfection of 1321N1 cells was used in the assessment of agonist potency at the P2X5 exon 10 receptor isoforms in the absence of P2X1 coexpression (Table 1). EC_{50} values of 0.3 and 12.2 μM for ATP and αβ-me-ATP, respectively, were observed in cells expressing P2X5FL alone. In contrast, upon transient expression of the P2X5Δ$^{328–349}$ isoform, neither ATP nor αβ-me-ATP displayed agonist activity up to the concentration of 100 μM.

Antagonist properties of PPADS, suramin, and TNP-ATP were measured in ATP-stimulated 1321N1 cells stably expressing P2X1, both alone and in combination with each of the P2X5 exon 10 isoforms (Table 1). Coexpression of P2X5FL increased the potency of TNP-ATP by 7-fold (IC_{50} = 0.12 μM)

TABLE 1
Pharmacological analysis of P2X1 and the P2X5 exon 10 isoforms in a FLIPR-based calcium assay
Not active means no significant increase in intracellular calcium in response to agonist application up to a concentration of 100 μM.

Channel	Agonists (EC_{50})		Antagonists (IC_{50})		
	ATP	αβ-me-ATP	PPADS	Suramin	TNP-ATP
			μM		
Parental 1321N1	Not active	Not active	Not determined	Not determined	Not determined
P2X1	0.057	0.160	0.21	1.17	0.89
P2X1/P2XFL5	0.072	0.150	0.09	1.79	0.12
P2X1/P2X5Δ$^{328–349}$	0.049	0.249	0.39	1.95	0.70
P2XFL5	0.3	12.2	0.65	13	2.5
P2X5Δ$^{328–349}$	Not active	Not active	Not determined	Not determined	Not determined

compared with its potency in the cell line expressing P2X1 alone (IC_{50} = 0.89 μM). The potencies of PPADS and suramin were not significantly affected by P2X5FL coexpression, and the potency of all three antagonists were unaffected by coexpression of P2X5$\Delta^{328–349}$.

P2X5FL, expressed alone after transient transfection, was sensitive to all three antagonists, whereas sensitivity of the P2X5$\Delta^{328–349}$ isoform could not be determined, because of the ATP nonresponsiveness of this receptor (Table 1).

Electrophysiological Analysis of the P2X5 Exon 10 Isoforms. ATP-induced currents were measured by whole-cell recordings in transiently transfected 1321N1 cells (Fig. 5). When P2X5FL was expressed in cells identified as transfectants by GFP expression, 30 μM ATP induced inward currents of more than 1 nA. In contrast, the same concentration of ATP produced inward currents of only approximately 10 pA in P2X5$\Delta^{328–349}$-expressing cells, a peak amplitude equivalent to that produced by 1321N1 cells expressing only the control GFP plasmid, demonstrating an absence of P2X5$\Delta^{328–349}$-specific ATP-evoked current.

Discussion

ATP plays a central role in cellular metabolism and energy trafficking, which are fundamental processes common among animal life forms. It should not be surprising, therefore, that the cell surface receptors that mediate the effects of ATP should be highly conserved. Despite considerable conservation of the amino acids encoded by exon 10 of the gene encoding P2X5, the expression of this protein is polymorphic in humans. A SNP located in the 3′ splice site of exon 10 leads not only to production of multiple forms of the protein, but to polymorphism for the expression of functional protein. Absence of the residues encoded by exon 10 results in a protein with an incomplete ATP binding domain and an incomplete second transmembrane domain, structural features that likely account for the apparent absence of function of this receptor isoform (Duckwitz et al., 2006).

Despite sample sizes that are smaller than those normally used for determining allele frequencies, it nonetheless can be concluded from our genotyping efforts that the P2X5$\Delta^{328–349}$-encoding allele is common, because it was the only allele found in three ethnic groups surveyed. Even in the ethnic group that showed polymorphism (African Americans), the P2X5$\Delta^{328–349}$-encoding allele was more common by a count of 12 to 8. Although our sample sizes are modest, our data set provides a noteworthy advancement in the understanding of P2X5 allele frequencies compared with the survey of 14 expressed sequence tag deposits reported by Bo et al. (2003) in their characterization of the polymorphism. Moreover, by determining the splice variants expressed by individuals of known genotype, we provide the first experimental corroboration of the functionality of the 3′ splice site of P2X5 exon 10; our results demonstrate a correlation that had been predicted, but not previously shown.

The predominance of exon 10-containing P2X5 transcripts in other mammalian species implies that the P2X5FL-encoding allele is ancestral. The Ensembl database provides no evidence of the exon 10 SNP in chimpanzees, strongly suggesting that mutation to the derived P2X5$\Delta^{328–349}$-encoding allele is of human origin. Although an allele aging analysis is outside the scope of this study, the predominance of the

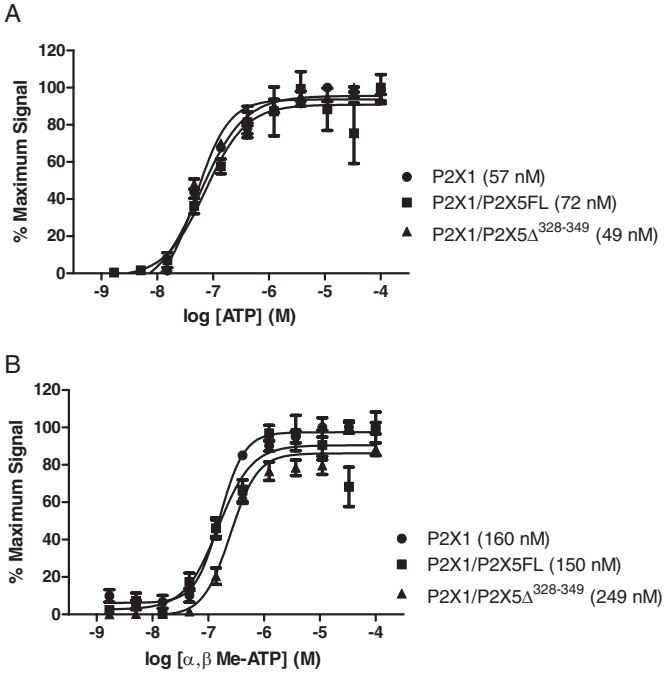

Fig. 4. Averaged traces from FLIPR-based assay of intracellular calcium. Functional activity of ATP and $\alpha\beta$-me-ATP at human purinergic receptors, as measured by FLIPR signal using Fluo-4 as a calcium indicator. The data were normalized to the signal maximum (defined as 100%). The points on each graph represent the mean ± S.E.M. of six to eight replicates. EC_{50} values are as indicated for each trace.

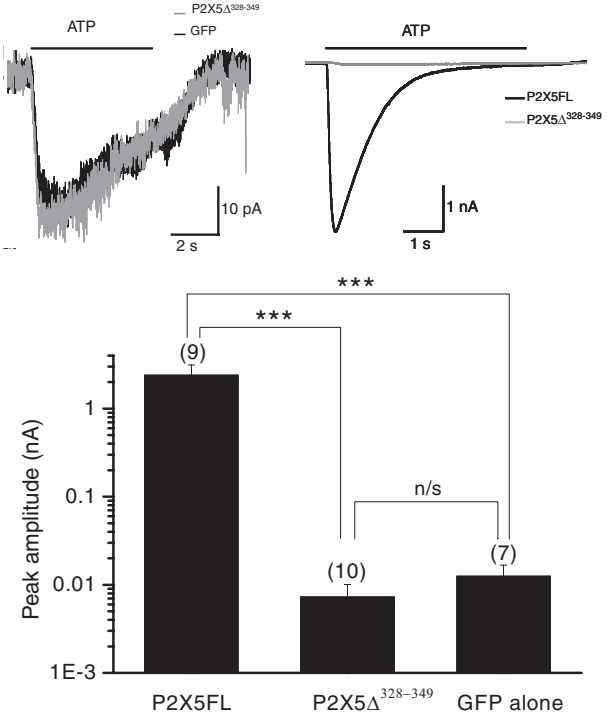

Fig. 5. Electrophysiological analysis of 1321N1 cells transiently expressing human P2X5 exon 10 isoforms. Top, current peak amplitudes were measured in response to 30 μM ATP infusion in 1321N1 cells and 1321N1 cells transiently coexpressing either P2X5FL, P2X5$\Delta^{328–349}$ with GFP (for identification of transfectants), or GFP alone (negative control). Bottom, means ± S.E.M. are graphed; group sample sizes are in parentheses. Log-transformed data were analyzed by single-classification analysis of variance followed by post hoc testing of all pairwise comparisons (Bonferroni method). n/s, not statistically significant; ***, $p < 0.001$.

derived allele in such diverse human populations as white Americans, Middle Easterners, and Chinese suggests an early human origin, dating to a time before the ecological radiation of human populations from Africa. Alternatively, but less likely, the SNP could have an origin that antedates human speciation, but with subsequent fixation of the P2X5FL-encoding allele in other hominid species.

Because P2X5 forms functional heteromeric channels with P2X1, our immunocytochemical analysis and pharmacological characterization focused on assessing the P2X5 isoforms coexpressed with P2X1 in stably expressing cell lines. Immunostaining of 1321N1 stably expressing cells indicates that P2X5FL resides at the cell surface, showing colocalization with P2X1, whereas P2X5$\Delta^{328-349}$ is cytoplasmic, despite the presence of one complete TM, suggestive of a correlation between function and localization. This finding, however, is in contrast with that of Lê et al. (1997), who observed cell surface expression of P2X5$\Delta^{328-349}$ in human embryonic kidney 293 cells. We chose 1321N1 cells for our heterologous expression because they lack endogenous ATP currents, an observation that has been reported (Jarvis et al., 2002; Nagata et al., 2009) and confirmed by our group. In addition, Lê et al. (1997) expressed the P2X5$\Delta^{328-349}$ isoform with a C-terminal FLAG epitope, whereas we expressed the native protein. It is unclear whether these differences contribute to our contrasting results. It should be noted that our observation of cytoplasmic P2X5$\Delta^{328-349}$ is in agreement with later work showing aggregation of this isoform (Duckwitz et al., 2006). In a *Xenopus laevis* oocyte expression system, not all residues encoded by exon 10 were required for cell surface expression. A construct (P2X5$\Delta^{342-349}$) lacking eight residues internal to TM2 was able to form trimeric assemblies in the membrane, a result that Duckwitz et al. (2006) interpreted to mean that the capacity to trimerize, rather than the presence of an intact TM, determines cellular localization. The P2X5$\Delta^{328-349}$ isoform, apparently lacking the capacity to trimerize even in the presence of its partner P2X1, would then be expected to be limited to the cytoplasm.

Rodent P2X5 coexpressed with P2X1 results in a pharmacological profile differing from that of either P2X1 or P2X5 expressed alone (Torres et al., 1998; Haines et al., 1999). Using a FLIPR-based calcium assay, we found that human P2X5FL coexpressed with P2X1 leads to a minimal change in agonist potency and a 7-fold increase in potency of the antagonist TNP-ATP. Although P2X1 and P2X5 are believed to heteromerize, our efforts to coimmunoprecipitate these receptors from our stably expressing cell lines were not successful (data not shown). In addition, attempts to colocalize P2X1 and P2X5 by immunostaining of human cardiac tissue were not successful; in these studies that used commercially available samples of unknown P2X5 genotype, an endothelial marker colocalized with P2X5 but not P2X1 (data not shown).

It is difficult to compare directly our pharmacological characterization and that of Lalo et al. (2008), because theirs was electrophysiological and ours used a fluorometric assay. In their study, coexpression of P2X5FL with P2X1 resulted in a functional output not easily predicted from the analysis of each receptor in isolation. Overall, our FLIPR studies of stably transfected 1321N1 cells indicate that the dominant driver of increases in intracellular calcium is P2X1, with at best small shifts in agonist potency resulting from coexpression of P2X5. When expressed alone, P2X5$\Delta^{328-349}$ showed no ATP- or $\alpha\beta$-me-ATP-mediated FLIPR signal, results consistent with our observation of cytoplasmic distribution of this isoform. Pharmacology of the antagonists PPADS and suramin at human P2X1 was essentially unaffected by coexpression of either P2X5 isoform. In addition, our electrophysiological assessment of the human P2X5 exon 10 isoforms showed a robust ATP-evoked signal from 1321N1 cells transiently expressing P2X5FL, but only background levels of current from cells expressing P2X5$\Delta^{328-349}$. Our electrophysiological analysis did not include coexpression of both P2X5 isoforms, which would have mimicked P2X5 expression in individuals heterozygous for the exon 10 SNP. However, the logical outcome of such an experiment would be signal-mediated by P2X5FL alone. Taken together, our results confirm previous reports that human P2X5FL can form a functional ATP-gated channel, but that P2X5$\Delta^{328-349}$ lacks such function.

The physiological consequences of the P2X5 exon 10 polymorphism are not known. In addition to being implicated in cell differentiation (Gröschel-Stewart et al., 1999; Meyer et al., 1999; Ryten et al., 2002), purinergic receptors are expressed in a variety of human tumor cell lines. ATP has been shown to be antineoplastic, with P2X5 being one of two P2X receptors (with P2X7) and three P2Y receptors possibly responsible for the observed ATP-mediated suppression of tumor growth (White and Burnstock, 2006; Shabbir and Burnstock, 2009). P2X5 is one of five purinergic receptors expressed in human basal cell carcinoma (BCC) and SCC tumor samples (Greig et al., 2003), although its role in the etiology of these cancers is unclear. Greig et al. (2003) found cytoplasmic P2X5 staining in BCC samples but cell surface staining in SCC samples (perhaps suggestive of functional P2X5), although in neither case was the sample's exon 10 genotype reported. Our genotyping and RT-PCR analysis of the A431 SCC cell line indicate these cells express the P2X5$\Delta^{328-349}$ isoform. Consistent with these findings, our immunocytochemical analysis of these cells indicates cytoplasmic P2X5 staining. The P2X5 antibody used by Greig et al. (2003), like ours, does not distinguish P2X5FL from P2X5$\Delta^{328-349}$. Nonetheless, our results are in stark contrast; Greig et al. (2003) observed cell surface expression of P2X5 in A431 cells. More extensive genotyping of BCC and SCC samples will allow a deeper investigation of the relationship between P2X5 isoform expression and subcellular location. Of greater importance, such genotyping will be required to establish what relationship, if any, exists between the isoform of P2X5 expressed and the incidence of these cancers.

Although the idea is only speculative, if P2X5 is a mediator of the antineoplastic activity attributed to ATP, individuals expressing functional P2X5 might be protected from the development of certain cancers. The incidence of skin cancer, including BCC and SCC, is substantially lower in African Americans than in white Americans, an observation that is most frequently attributed to the UV-protective properties of melanin (Halder and Bridgeman-Shah, 1995; Kabigting et al., 2009). That this skin pigmentation protein can modulate the damaging effects of UV radiation is well established, but does not rule out the existence of other genetic factors at play. Expression of P2X5FL, with its putative antineoplastic function, is worthy of consideration as a possible genetic contributor to lower rates of skin cancer in African Americans.

Maintenance of the P2X5FL-encoding allele in humans

might be explained by antineoplastic effects or other functions that have been attributed to the intact receptor. More difficult to reconcile is the predominance of the allele encoding P2X5$\Delta^{328-349}$. Future studies will need to be directed toward determining what selective forces, directional or balancing, might be acting at this locus and determining the state of linkage disequilibrium within the surrounding chromosomal region. One possibility is that the P2X5 exon 10 polymorphism is not under direct selection. Rather, selection might be acting at a nearby locus, with the P2X5$\Delta^{328-349}$-encoding allele displaying strong linkage disequilibrium with an allele that is favored by selection.

Our intent with this article is to stimulate more expansive genetic and molecular analyses of this polymorphism. More extensive P2X5 genotyping in the human population is in order, including analysis of additional ethnic and geographically distinct populations. Although it remains unclear what evolutionary forces have been responsible for the high frequency of nonfunctional P2X5 receptor that we currently observe in humans, the existence of this polymorphism provides an unusual opportunity to investigate selective forces at work within our species.

Acknowledgments

We thank Dr. Jody Hey for beneficial suggestions; Drs. Gustave Hebert and Erik Charych for immunocytochemistry expertise; and Deborah L. Smith and Dr. Catherine Bingham for critical reading of the manuscript.

References

Ashour F, Atterbury-Thomas M, Deuchars J, and Evans RJ (2006) An evaluation of antibody detection of the P2X1 receptor subunit in the CNS of wild type and P2X1-knockout mice. *Neurosci Lett* **397:**120–125.
Bo X, Jiang LH, Wilson HL, Kim M, Burnstock G, Surprenant A, and North RA (2003) Pharmacological and biophysical properties of the human P2X5 receptor. *Mol Pharmacol* **63:**1407–1416.
Burnstock G (2006) Purinergic signalling. *Br J Pharmacol* **147:**S172–S181.
Cherry J, Nieuwenhuijsen BW, Kaftan EJ, Kennedy JD, and Chanda PK (2008) A modified method for PCR-directed gene synthesis from large number of overlapping oligodeoxyribonucleotides. *J Biochem Biophys Methods* **70:**820–822.
Cockayne DA, Dunn PM, Zhong Y, Rong W, Hamilton SG, Knight GE, Ruan HZ, Ma B, Yip P, Nunn P, et al. (2005) P2X2 knockout mice and P2X2/P2X3 double knockout mice reveal a role for the P2X2 receptor subunit in mediating multiple sensory effects of ATP. *J Physiol* **567:**621–639.
Collo G, North RA, Kawashima E, Merlo-Pich E, Neidhart S, Surprenant A, and Buell G (1996) Cloning of P2X5 and P2X6 receptors and the distribution and properties of an extended family of ATP-gated ion channels. *J Neurosci* **16:**2495–2507.
Cox JA, Barmina O, and Voigt MM (2001) Gene structure, chromosomal localization, cDNA cloning and expression of the mouse ATP-gated ionotropic receptor P2X5 subunit. *Gene* **270:**145–152.
Diaz-Hernandez M, Cox JA, Migita K, Haines W, Egan TM, and Voigt MM (2002) Cloning and characterization of two novel zebrafish P2X receptor subunits. *Biochem Biophys Res Commun* **295:**849–853.
Duckwitz W, Hausmann R, Aschrafi A, and Schmalzing G (2006) P2X5 subunit assembly requires scaffolding by the second transmembrane domain and a conserved aspartate. *J Biol Chem* **281:**39561–39572.
Garcia-Guzman M, Soto F, Laube B, and Stühmer W (1996) Molecular cloning and functional expression of a novel rat heart P2X purinoceptor. *FEBS Lett* **388:**123–127.
Greig AV, Linge C, Healy V, Lim P, Clayton E, Rustin MH, McGrouther DA, and Burnstock G (2003) Expression of purinergic receptors in non-melanoma skin cancers and their functional roles in A431 cells. *J Invest Dermatol* **121:**315–327.
Gröschel-Stewart U, Bardini M, Robson T, and Burnstock G (1999) Localisation of P2X5 and P2X7 receptors by immunohistochemistry in rat stratified squamous epithelia. *Cell Tissue Res* **296:**599–605.
Guo C, Masin M, Qureshi OS, and Murrell-Lagnado RD (2007) Evidence for functional P2X4/P2X7 heteromeric receptors. *Mol Pharmacol* **72:**1447–1456.
Guo W, Xu X, Gao X, Burnstock G, He C, and Xiang Z (2008) Expression of P2X5 receptors in the mouse CNS. *Neuroscience* **156:**673–692.
Haines WR, Torres GE, Voigt MM, and Egan TM (1999) Properties of the novel ATP-gated ionotropic receptor composed of the P2X(1) and P2X(5) isoforms. *Mol Pharmacol* **56:**720–727.
Halder RM and Bridgeman-Shah S (1995) Skin cancer in African Americans. *Cancer* **75:**667–673.
Hansen MA, Barden JA, Balcar VJ, Keay KA, and Bennett MR (1997) Structural motif and characteristics of the extracellular domain of P2X receptors. *Biochem Biophys Res Commun* **236:**670–675.
International HapMap Consortium (2003) The International HapMap Project. *Nature* **426:**789–796.
Jarvis MF, Burgard EC, McGaraughty S, Honore P, Lynch K, Brennan TJ, Subieta A, Van Biesen T, Cartmell J, Bianchi B, et al. (2002) A-317491, a novel potent and selective non-nucleotide antagonist of P2X3 and P2X2/3 receptors, reduces chronic inflammatory and neuropathic pain in the rat. *Proc Natl Acad Sci USA* **99:**17179–17184.
Jensik PJ, Holbird D, Collard MW, and Cox TC (2001) Cloning and characterization of a functional P2X receptor from larval bullfrog skin. *Am J Physiol Cell Physiol* **281:**C954–C962.
Kabigting FD, Nelson FP, Kauffman CL, Popoveniuc G, Dasanu CA, and Alexandrescu DT (2009) Malignant melanoma in African-Americans. *Dermatol Online J* **15:**3.
Kawate T, Michel JC, Birdsong WT, and Gouaux E (2009) Crystal structure of the ATP-gated P2X(4) ion channel in the closed state. *Nature* **460:**592–598.
Lalo U, Pankratov Y, Wichert SP, Rossner MJ, North RA, Kirchhoff F, and Verkhratsky A (2008) P2X1 and P2X5 subunits form the functional P2X receptor in mouse cortical astrocytes. *J Neurosci* **28:**5473–5480.
Lê KT, Boué-Grabot E, Archambault V, and Séguéla P (1999) Functional and biochemical evidence for heteromeric ATP-gated channels composed of P2X1 and P2X5 subunits. *J Biol Chem* **274:**15415–15419.
Lê KT, Paquet M, Nouel D, Babinski K, and Séguéla P (1997) Primary structure and expression of a naturally truncated human P2X ATP receptor subunit from brain and immune system. *FEBS Lett* **418:**195–199.
MacKenzie AB, Surprenant A, and North RA (1999) Functional and molecular diversity of purinergic ion channel receptors. *Ann NY Acad Sci* **868:**716–729.
Meyer MP, Gröschel-Stewart U, Robson T, and Burnstock G (1999) Expression of two ATP-gated ion channels, P2X5 and P2X6, in developing chick skeletal muscle. *Dev Dyn* **216:**442–449.
Musa H, Tellez JO, Chandler NJ, Greener ID, Maczewski M, Mackiewicz U, Beresewicz A, Molenaar P, Boyett MR, and Dobrzynski H (2009) P2 purinergic receptor mRNA in rat and human sinoatrial node and other heart regions. *Naunyn Schmiedebergs Arch Pharmacol* **379:**541–549.
Nagata K, Imai T, Yamashita T, Tsuda M, Tozaki-Saitoh H, and Inoue K (2009) Antidepressants inhibit P2X4 receptor function: a possible involvement in neuropathic pain relief. *Mol Pain* **5:**20.
Nicke A (2008) Homotrimeric complexes are the dominant assembly state of native P2X7 subunits. *Biochem Biophys Res Commun* **377:**803–808.
North RA (2002) Molecular physiology of P2X receptors. *Physiol Rev* **82:**1013–1067.
Ruppelt A, Ma W, Borchardt K, Silberberg SD, and Soto F (2001) Genomic structure, developmental distribution and functional properties of the chicken P2X(5) receptor. *J Neurochem* **77:**1256–1265.
Ryten M, Dunn PM, Neary JT, and Burnstock G (2002) ATP regulates the differentiation of mammalian skeletal muscle by activation of a P2X5 receptor on satellite cells. *J Cell Biol* **158:**345–355.
Shabbir M and Burnstock G (2009) Purinergic receptor-mediated effects of adenosine 5′-triphosphate in urological malignant diseases. *Int J Urol* **16:**143–150.
Surprenant A and North RA (2009) Signaling at purinergic P2X receptors. *Annu Rev Physiol* **71:**333–359.
Torres GE, Haines WR, Egan TM, and Voigt MM (1998) Co-expression of P2X1 and P2X5 receptor subunits reveals a novel ATP-gated ion channel. *Mol Pharmacol* **54:**989–993.
Virginio C, North RA, and Surprenant A (1998) Calcium permeability and block at homomeric and heteromeric P2X2 and P2X3 receptors, and P2X receptors in rat nodose neurones. *J Physiol* **510:**27–35.
White N and Burnstock G (2006) P2 receptors and cancer. *Trends Pharmacol Sci* **27:**211–217.

Address correspondence to: Garth T. Whiteside, Pfizer Global Research and Development, CN8000, Princeton, NJ 08543-8000. E-mail: whitesg@wyeth.com